Available online at www.sciencedirect.com
SCIENCE DIRECT®
ELSEVIER
International Journal of Solids and Structures 43 (2006) 4342–4356
INTERNATIONAL JOURNAL OF SOLIDS and STRUCTURES
www.elsevier.com/locate/ijsolstr

Maximum frequency design of laminated plates with mixed boundary conditions

Yoshihiro Narita *

Department of Mechanical Engineering, School of Engineering, Hokkaido University, N13, W8, Kita-ku, Sapporo 060-8628, Japan

Received 8 March 2005
Available online 23 September 2005

Abstract

A layerwise optimization (LO) approach is extended to accommodate the finite element analysis for optimizing the free vibration behavior of laminated composite plates with discontinuities along the boundaries. The classical non-conforming finite element is modified to fit into the LO procedure and is used to calculate natural frequencies of symmetrically laminated plates. This combined LO-FEM approach is applied to laminated rectangular plates with combinations of free, simply supported and clamped edges along parts of the plate boundary. The fundamental frequency, an object function for the present study, is maximized by optimizing design variables that are a set of fiber orientation angles in the layers. For illustrative purpose nine examples of square and rectangular plates with various types of mixed boundary conditions are considered, and a comprehensive set of results are presented for the optimum fiber orientation angles and the maximum fundamental frequencies of the 8-layer and 24-layer plates.

Keywords: Optimum design; Natural frequency; Laminated plate; Composites; Mixed boundary condition

1. Introduction

The use of fibrous composites is rapidly increasing in structural applications and there arises a vast demand for information on the vibration characteristics of composite structural elements. Among them, a laminated rectangular plate having discontinuities along the boundary constitutes an important problem, since laminated composites in practical applications are constrained in various fashion along the edges.

A literature survey shows that the vibration of *isotropic* plates with mixed boundary conditions has been analyzed in a number of references. Ohta and Hamada (1963) obtained the fundamental frequency of a

* Fax: +81 11 706 7889.
E-mail address: ynarita@eng.hokudai.ac.jp

0020-7683/$ - see front matter © 2005 Elsevier Ltd. All rights reserved.
doi:10.1016/j.ijsolstr.2005.06.104

simply supported plate partially clamped on the edge. Keer and Stahl (1972) analyzed the problem by use of a Fredholm integral equation and showed variation of the fundamental frequency with the change of clamped portion. This problem was also studied by Rao et al. (1973) by making use of the finite element method. These works are limited to determining the fundamental frequencies.

In the 1980s, the present author (Narita, 1981) published a paper to extend a series-type method to vibration of orthotropic rectangular plates and presented the lowest several frequencies. Fan and Cheung (1984) used a finite strip method to analyze rectangular plates with complex edge support conditions. Gorman (1984) applied an accurate series-type approach to the analysis of rectangular plates with mixed boundary conditions.

More recently, in the 1990s, Mizusawa and Leonard (1990) used a spline strip method to study vibration and buckling of plates with mixed boundary conditions. Liew et al. (1993) applied the substructure method to the problem. Laura and Gutierrez (1994) analyzed vibrating rectangular plates with non-uniform boundary conditions by using the differential quardrature (DQ) method. Shu and Wang (1999) treated mixed and non-uniform boundary conditions in generalized differential quadrature (GDQ) analysis. Wei et al. (2001) determined natural frequencies of rectangular plates with mixed boundary conditions by using discrete singular convolution.

Despite such previous studies for isotropic case, a lack of solutions is obvious for the vibration of *composite* plates with mixed boundary conditions. Moreover, to the author's best knowledge, there are no papers dealing with the optimization problem of vibrating laminated composite plates having mixed boundary conditions, although some papers are found, for example a work by Fukunaga et al. (1994) using the lamination parameters (Gurdal et al., 1999), to deal with vibration optimization of laminate plates with uniform boundary conditions.

The primary objectives of this paper are to develop a finite element to be implemented in the layerwise optimization (LO) approach and to apply the LO-FEM approach to the frequency design problem for laminated composite plates with mixed boundary conditions. The LO approach was first proposed by the present author (Narita, 2003) to determine the maximum fundamental frequency of laminated composite plates and was improved as a more general iterative approach (Narita and Turvey, 2004). In these previous papers, a Ritz method was used to calculate the object function, viz a fundamental frequency of the plate. The Ritz method has an advantage in its efficient computation for plates with *uniform* edges, but is not suitable for dealing with more complicated problems such as the plates with mixed boundary conditions, as considered in the present paper.

In this work, a classical non-conforming finite element is modified to be used in the LO procedure for symmetrically laminated composite plates. The combined LO-FEM approach is applied to thin laminated rectangular plates with combinations of free, simply supported and clamped partial edges. The fundamental frequency is maximized by use of design variables that are a set of fiber orientation angles in the layers. Nine examples of square and rectangular plates are considered with various types of mixed boundary conditions, and results are presented for the optimum fiber orientation angles and the corresponding maximum fundamental frequencies of the symmetric 8-layer and 24-layer plates.

2. Optimum design problem and LO procedure

2.1. Problem description

A symmetrically laminated rectangular plate is considered, as shown in Fig. 1, where in each layer the major and minor principal material axes are denoted by the L and T axes, respectively. The E_L and E_T are elastic moduli in the L and T directions, respectively, G_{LT} is the shear modulus and v_{LT} is the major Poisson

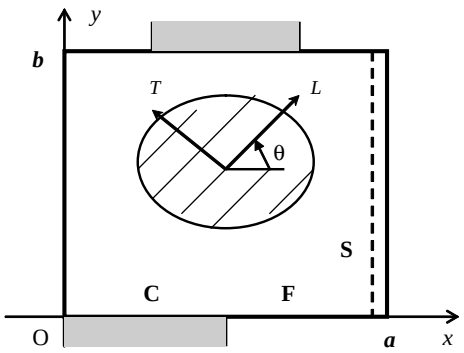

Fig. 1. Laminated composite rectangular plate with mixed boundary conditions.

ratio. The angle between the L and x axes is denoted by θ. The total number of layers is $2K$, where K layers exist in the upper (lower) half of cross-section.

The dimension of the whole plate is given by $a \times b \times h$ (plate thickness). The plate has mixed boundary conditions, specifically having free, simply supported and clamped edges along parts of the boundary. The symbols F, S and C stand for free, simply supported and clamped edges, respectively, and are used in the way as marked in Fig. 1.

For laminated thin plates, the motion of the plate vibrating in sinusoidal time variation is governed by

$$D_{11}\frac{\partial^4 w}{\partial x^4} + 2(D_{12} + 2D_{66})\frac{\partial^4 w}{\partial x^2 \partial y^2} + D_{22}\frac{\partial^4 w}{\partial y^4} + 4D_{16}\frac{\partial^4 w}{\partial x^3 \partial y} + 4D_{26}\frac{\partial^4 w}{\partial x \partial y^3} - \rho\omega^2 w = 0 \tag{1}$$

where w is the amplitude, ρ is a mean mass per unit area of the plate and ω is a radian frequency of free vibration. The D_{pq} $(p, q = 1, 2, 6)$ are the bending stiffness of the symmetric laminate and are determined in the lamination theory (Vinson and Sierakowski, 1986; Jones, 1999) by

$$D_{pq} = \frac{2}{3}\sum_{k=1}^{K} \overline{Q}_{pq}^{(k)}(z_k^3 - z_{k-1}^3) \tag{2}$$

$(p, q = 1, 2, 6)$, where z_k is a thickness coordinate measured from the middle surface. The $\overline{Q}_{pq}^{(k)}$ are elastic constants in the kth layer and are defined by E_L, E_T, G_{LT} and v_{LT}, together with the fiber orientation angle θ.

Natural frequency is normalized as a frequency parameter

$$\Omega = \omega a^2(\rho/D_0)^{1/2} \tag{3}$$

where $D_0 = E_T\, h^3/12(1 - v_{LT}v_{TL})$ is a reference bending stiffness. The frequency parameter Ω_1 for the fundamental (lowest) mode is used as an object function and will be designed to maximize its value in the present optimization. The mathematical expression for such optimization problem is written as

$$\Omega_1 = \Omega_1(\vec{\theta}) \to \text{Max} \quad \text{(object function)} \tag{4}$$

subject to

$$\begin{aligned} &\vec{\theta} = (\theta_1, \theta_2, \ldots, \theta_K) \quad \text{(design variables)} \\ &-90^\circ \leqslant \theta_k \leqslant 90^\circ \quad (k = 1, 2, \ldots, K) \quad \text{(constraint conditions)} \end{aligned} \tag{5}$$

The design variables are taken to be a set of fiber orientation angles in the K layers of the half of the cross-section and are written in the notation

$$[\theta_1/\theta_2/\cdots/\theta_k/\cdots/\theta_K]_S \tag{6}$$

where θ_k is an fiber orientation angle in the kth layer ($k = 1$: outermost, $k = K$: innermost) and a subscript "s" denotes a symmetric lamination. The angles are hereafter given only by numbers for the sake of brevity, i.e. $[-45/90]_s$ instead of $[-45°/90°]_s$.

2.2. Layerwise optimization (LO) procedure

When a fiber orientation angle in each layer is taken to be a design variable in one-to-one way, an intensive computational problem is unavoidable, wherein optimum solutions must be determined in multi-dimensional space. One way to avoid such a computational problem is to use the lamination parameters (Gurdal et al., 1999). The use of such intermediate parameters, however, requires another mathematical process which prevents practical use of the approach from obtaining the actual optimum fiber orientation angles.

The LO approach dissolves such a conventional mathematical and/or computational problem and reduces the multi-dimensional optimum solution search to a few iterative cycles of one-dimensional search (Narita and Turvey, 2004). For such significant reduction, physical observation that the outer layer has more stiffening effect than the inner layer in bending of laminated plates is utilized. This well-known physical fact may be interpreted as "the outer layer plays more decisive role in determining the natural frequency of laminated plates". Based on this observation, a hypothesis that

The optimum stacking sequence $[\theta_1/\theta_2/\cdots/\theta_k/\cdots/\theta_K]_{s,\mathrm{opt}}$ *for the maximum natural frequency of laminated plates can be determined sequentially in the order from the outermost to the innermost layer* is proposed.

Suppose $\Omega^{(k)}_{1,\mathrm{opt}}$ is assumed to be the maximum frequency parameter obtained in the kth step (Note that the same k indicating the layer number is used because it deals with the kth layer), the following procedure, based on the foregoing assumption, is used to determine the maximum fundamental frequency $\Omega_{1,\mathrm{opt}}$.

Step 0. Assume a symmetrically laminated plate made of K hypothetical layers in the half of the cross-section with *no bending stiffness*.
Step 1. Find $\theta_{1,\mathrm{opt}}$, using a one-dimensional search, which gives $\Omega^{(1)}_{1,\mathrm{opt}}$ to maximize the object function of the laminated plate with an orthotropic lamina (i.e., with E_L, E_T, G_{LT} and v_{LT}) in the first (outermost) layer. The $(K-1)$ inner layers remain hypothetical with no bending stiffness.
Step 2. Find $\theta_{2,\mathrm{opt}}$, using a one-dimensional search, which gives $\Omega^{(2)}_{1,\mathrm{opt}}$ of the laminated plate with an orthotropic lamina in the second layer and an orthotropic first layer with $\theta_1 = \theta_{1,\mathrm{opt}}$. The inner $(K-2)$ layers remain hypothetical with no stiffness.
Step k ($k = 3$ to $K-1$). The foregoing process is repeated to yield $\theta_{3,\mathrm{opt}},\ldots\theta_{(K-1),\mathrm{opt}}$.
Step K. Find $\theta_{K,\mathrm{opt}}$ which gives $\Omega^{(K)}_{1,\mathrm{opt}}$ to maximize the object function of the laminated plate with an orthotropic lamina in the Kth innermost layer. This last step determines the optimum lay-up $[\theta_1/\theta_2/\cdots/\theta_K]_{s,\mathrm{opt}}$ which yields the maximum object function $\Omega_{1,\mathrm{opt}} = \Omega^{(K)}_{1,\mathrm{opt}}$ of the plate.

The above set of *Steps* 1–K may be considered as one cycle of an LO iterative solution procedure. In the first cycle, the inner layers are initially assumed to have zero stiffness. The fiber orientation angles determined at *Step K* in the first cycle are considered as a better initial approximation for the second cycle.

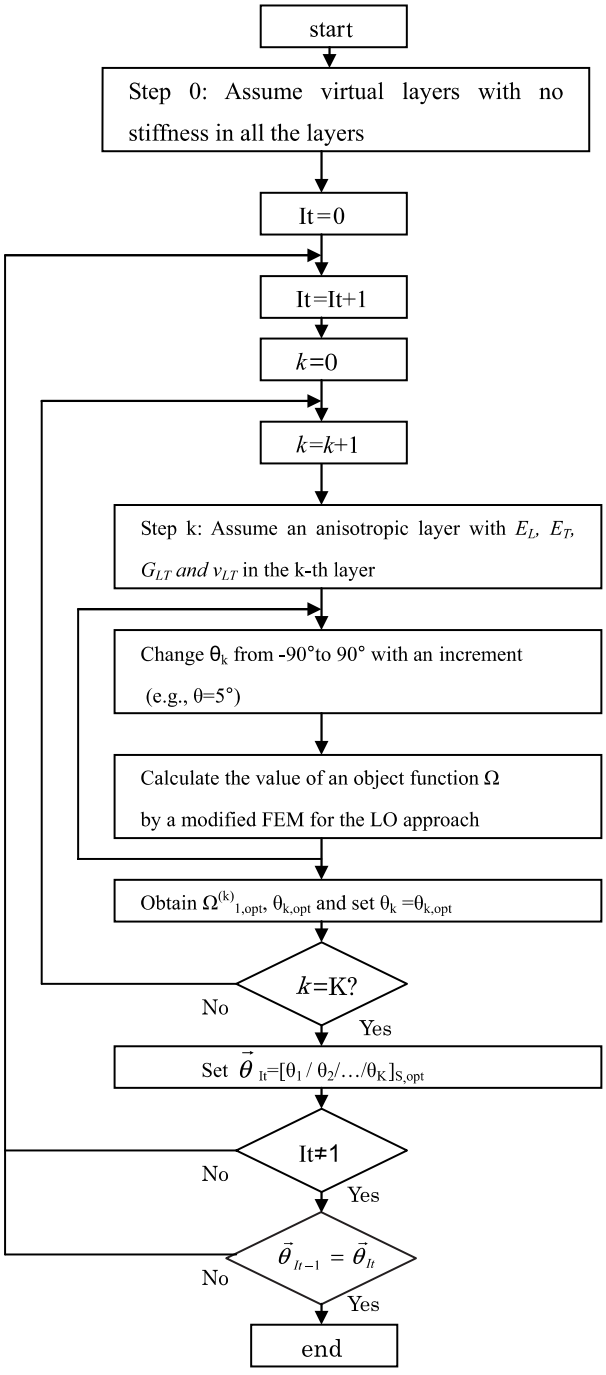

Fig. 2. Flow chart of the algorithm used in the LO approach.

The iterative cycles continue until a converged solution is obtained. The algorithm is described in the flow chart in Fig. 2.

2.3. Finite element formulation modified in LO procedure

Due to the difficulty in solving the differential equation (1) that involves odd derivatives, the direct analytical solution is impractical, particularly for problems involving *mixed* boundary conditions. The finite element method is therefore employed to consider such complicating edge conditions. For symmetrically laminated thin plates, the strain energy stored in the plate during bending is given by

$$U = \frac{1}{2}\iint_A \{\kappa\}^{\mathrm{T}}[D]\{\kappa\}\,\mathrm{d}A \tag{7}$$

where

$$\{\kappa\} = \left\{ -\frac{\partial^2 w}{\partial x^2} \quad -\frac{\partial^2 w}{\partial y^2} \quad -2\frac{\partial^2 w}{\partial x \partial y} \right\}^{\mathrm{T}} \tag{8}$$

is a vector of bending curvatures, consisting of second derivatives of w, and $[D]$ is the bending stiffness coefficient matrix

$$[D] = \begin{bmatrix} D_{11} & D_{12} & D_{16} \\ D_{12} & D_{22} & D_{26} \\ D_{16} & D_{26} & D_{66} \end{bmatrix} \tag{9}$$

that relates the moment resultant

$$\{M\} = \{\, M_x \quad M_y \quad M_{xy} \,\}^{\mathrm{T}} \tag{10}$$

to the curvature (8) by the relationship $\{M\} = [D]\{\kappa\}$.

In applying the aforementioned LO approach, the stiffness element in Eq. (9) is modified from Eq. (2) to a form suited for use in *Step k* in the LO procedure as

$$D_{pq} = \frac{2}{3}\sum_{n=1}^{k} \overline{Q}_{pq}^{(n)}(z_n^3 - z_{n-1}^3) \tag{11}$$

$(p, q = 1, 2, 6)$, where the summation index n runs through from 1 to k and the stiffness evaluation for layers with $n = k+1$ to K is ignored. This means that the bending stiffness is evaluated in the outer k layers $(n = 1, \ldots, k)$ but is kept zero for hypothetical layers $(n = k+1, \ldots, K)$.

Suppose a rectangular finite element with nodes i, j, k, l and the deflection (amplitude) in the element is expressed (Zienkiewicz and Taylor, 1991) by

$$w(x, y) = [N]\{d_e\} \tag{12}$$

where $\{d_e\}$ is the element displacement vector

$$\{d_e\} = \{d_i, d_j, d_k, d_l\}^{\mathrm{T}} \tag{13}$$

obtained by listing four nodal displacement vectors such as

$$\{d_i\} = \{\, w_i \quad \partial w_i/\partial x \quad \partial w_i/\partial y \,\} \tag{14}$$

The shape function $[N]$ is written as

$$[N] = \{P\}[C]^{-1} \tag{15}$$

where $\{P\}$ and $[C]$ are defined by using

$$w(x, y) = \{P\}\{\alpha\} \tag{16}$$

$$\{P\} = \{\, 1 \quad x \quad y \quad x^2 \quad xy \quad y^2 \quad x^3 \quad x^2y \quad xy^2 \quad y^3 \quad x^3y \quad xy^3 \,\} \tag{17}$$

$$\{\alpha\} = \{\alpha_1, \alpha_2, \alpha_3, \ldots, \alpha_{12}\}^{\mathrm{T}} \tag{18}$$

and

$$\{d_e\} = [C]\{\alpha\} \tag{19}$$

The curvature vector is obtained by

$$\{\kappa\} = [Q]\{\alpha\} = [Q][C]^{-1}\{d_e\} \tag{20}$$

where $[Q]$ is derived from Eqs. (8) and (16). Substitution of Eq. (20) into Eq. (7) yields the strain energy

$$U_e = \frac{1}{2}\{d_e\}^{\mathrm{T}}[K_e]\{d_e\} \tag{21}$$

written in terms of the element displacement vector, where

$$[K_e] = ([C]^{-1})^{\mathrm{T}} \cdot \iint_A [Q]^{\mathrm{T}}[D][Q]\,\mathrm{d}A \cdot [C]^{-1} \tag{22}$$

is the element stiffness matrix in the present formulation.

Following similar procedure, the maximum kinetic energy of the plate element

$$T_e = \frac{1}{2}\omega^2 \iint_A \rho w^2\,\mathrm{d}A \tag{23}$$

may be rewritten in terms of the element displacement vector as

$$T_e = \frac{1}{2}\omega^2\{d_e\}^{\mathrm{T}}[M_e]\{d_e\} \tag{24}$$

where

$$[M_e] = ([C]^{-1})^{\mathrm{T}} \cdot \iint_A \rho w^2\,\mathrm{d}A \cdot [C]^{-1} \tag{25}$$

is the element mass matrix. As in the standard finite element procedure, one obtains the global eigenvalue equation as

$$([K] - \Omega^2[M])\{d\} = 0 \tag{26}$$

where $[K]$ and $[M]$ are the global stiffness and mass matrices, respectively, and $\{d\}$ is a global displacement vector. Eq. (26) is a set of homogeneous linear equations in the unknown displacements $\{d\}$. For non-trivial solution the determinant is equal to zero, and the eigenvalues correspond to natural frequencies of the plate. The lowest of these is used as an object function in the optimization.

3. Numerical results and discussions

3.1. Convergence and comparison of the FEM solutions

Numerical examples are given for symmetrically laminated, 8-layer or 24-layer square ($a/b = 1$) and rectangular plates ($a/b = 1/3$–3). The design variables are presented in the usual notation as $[\theta_1/\theta_2/\theta_3/\theta_4]_s$ for 8-layer plates, where θ_1 is the fiber orientation angle of the 1st layer (outermost) and θ_4 is that of the 4th layer (innermost). Each of the optimum fiber orientation angles for θ_1, θ_2, θ_3 and θ_4 is determined with an

increment of $\theta = 5°$ in one-dimensional search. The similar notation is used for 24-plates, as an example of plates with many layers, with an increment of $\theta = 15°$ in numerical results.

Boundary conditions are given for free (F), simply supported (S) and clamped (C) edges along parts of the plate boundary. For free edge part, no constraints are given to the displacement (16) and for simply supported edge part, amplitude w and slope parallel to the edge are rigidly constrained. All the elements in the nodal displacement vector (14) are set to zero along the clamped part. The elastic material constants used in the following examples are taken from a reference (Vinson and Sierakowski, 1986) as

$$\text{Graphite/epoxy } (G/E): \quad E_L = 138 \text{ GPa}, \quad E_T = 8.96 \text{ GPa}, \quad G_{LT} = 7.1 \text{ GPa}, \quad \nu_{LT} = 0.30 \tag{27}$$

for Graphite/epoxy composite with strong orthotropy ($E_L/E_T = 15.4$).

Fig. 3 presents nine numerical examples considered in the present study. They are classified into three groups with three examples each. In the first group (Ex. 1, 2, 3) plates are clamped only at one half ($a/2$) of a bottom edge while in the second group (Ex. 4, 5, 6) plates are clamped symmetrically at one half ($a/2$) of a pair of opposite edges. The plates are clamped in the third group (Ex. 7, 8, 9) symmetrically at four corners with a quarter length ($a/4$) of the edges. The total length of the clamped parts is therefore $a/2$, a and $2a$ for the first, second and third groups, respectively, in the case of square. The remaining edges, other than the clamped parts, are kept free in Ex. 1, 4, and 7 and are simply supported in Ex. 2, 5 and 8. The right-hand-side edge is simply supported and the rests are free in Ex. 3, 6 and 9.

A sample convergence study is presented in Table 1 for 8-layer square plates. The first five frequency parameters defined in Eq. (3) of Ex. 1 and Ex. 2 are given with different numbers of finite elements, starting

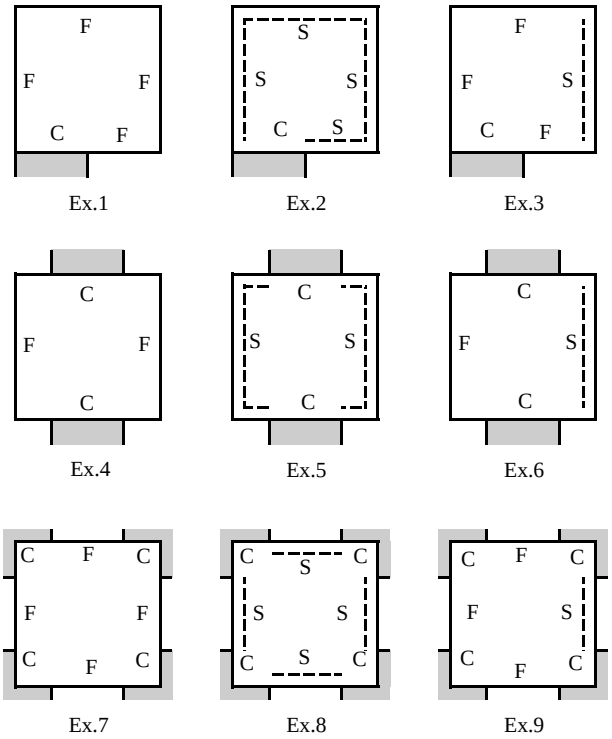

Fig. 3. Numerical examples—rectangular plates with mixed boundary conditions.

Table 1
Convergence study of lowest five frequency parameters Ω of 8-layer square plates ($a/b = 1$, $[30/-30/30/-30]_s$)

	Ω_1	Ω_2	Ω_3	Ω_4	Ω_5
Ex. 1					
14×14	4.419	16.55	27.58	45.48	72.80
16×16	4.428	16.51	27.53	45.37	72.72
18×18	4.422	16.49	27.51	45.31	72.69
20×20	4.398	16.47	27.51	45.28	72.69
Ex. 2					
14×14	56.54	111.9	148.7	187.2	219.4
16×16	56.57	112.0	148.8	187.4	219.8
18×18	56.59	112.0	148.9	187.5	220.1
20×20	56.61	112.1	149.0	187.7	220.3

from 14×14 to 20×20, in x and y directions. The fiber orientation angles are taken to $[30/-30/30/-30]_s$. Because the present finite element is a non-conforming element, there is no concrete tendency in frequency variation such as monotonous increase or decrease. Actually the frequencies generally decrease in Ex. 1 while they increase in Ex. 2 as the number of finite elements is increased. In any case it is observed that the frequency parameters are well converged for the present purpose, and the 20×20 solution will be used throughout in the paper.

There have been many papers dealing with vibration of *isotropic* plates with mixed boundary conditions and a comparison study is given in Table 2 for Ex. 2, 5 and 8 to verify the accuracy of the present FEM solution. There is no exact solution available for the problem. When the present result $\Omega_1 = 22.49$ in Ex. 2 is compared to the average value $\Omega_1 = 22.51$ of the other 11 past reference values, they are found in very good agreement (difference is less than 0.1%). The same is true (about 0.4% difference) when Ex. 5 for $\Omega_1 = 28.37$ is compared to the average values of $\Omega_1 = 28.49$ of the other five results. The agreement between the present FEM and other results is thus quite excellent, even up to higher modes. Table 3 presents the first five frequencies of Ex. 1, 3, 4, 6, 7 and 9 of isotropic square plates for future comparisons, where no reference values have been found so far.

3.2. Optimum solutions for square and rectangular plates

Table 4 presents one example of the optimization process for a square plate (Ex. 2) when the number of iterative cycles (NIC) is two for complete convergence with an increment $\theta = 5°$ in one-dimensional search. The first cycle, composed of five steps in the case of symmetric 8-layer plate, yields the optimum design variables (a set of the fiber orientation angles) of [70/−50/50/50]s with $\Omega_1 = 62.32$. The fiber orientation angles thus obtained are used as a starting solution (Step 0) in the second cycle, and the second cycle ends up with [55/−50/−55/55] and $\Omega_1 = 63.54$. The third cycle gives an identical solution as in the second cycle, indicating that the solution is converged within the span of an increment $\theta = 5°$.

Table 5 presents a list of converged optimum solutions for the nine examples of square plates obtained by an LO procedure. To each example, the optimum fiber orientation angle $[\theta_1/\theta_2/\theta_3/\theta_4]_{s,\mathrm{opt}}$ and the corresponding maximum fundamental frequency $\Omega_{1,\mathrm{opt}}$ are given with the number of iterative cycles (NIC). There are no specific fiber orientation angles that are dominant in the first (Ex. 1–3) and second groups (Ex. 4–6), but the dominant angles $\pm 45°$ are found in the third group (Ex. 7–9) due to the strong clamping constraints symmetrically located in the four corners. NIC = 1 was found in four examples among nine examples.

Table 6 is used to verify that the optimum solutions $[\theta_1/\theta_2/\theta_3/\theta_4]_{s,\mathrm{opt}}$ listed in Table 5 actually give higher frequency values than those with other stacking sequences. Typical stacking sequences of the

Table 2
Comparison of frequency parameters Ω of *isotropic* square plates with mixed boundary conditions ($\nu = 0.3$)

	Ω_1	Ω_2	Ω_3	Ω_4	Ω_5
Ex. 2					
Present FEM	22.49	49.84	55.62	81.85	99.43
Ohta and Hamada (1963)	22.4	–	–	–	–
Keer and Stahl (1972)	22.49	–	–	–	–
Rao et al. (1973)	22.96	–	–	–	–
Narita (1981)	22.63	50.04	55.95	82.34	99.71
Fan and Cheung (1984)	22.73	50.15	56.23	–	–
Gorman (1984)	22.48	–	–	–	–
Mizusawa and Leonard (1990)	22.71	50.10	56.13	82.37	99.73
Liew et al. (1993)	22.40	–	–	–	–
Laura and Gutierrez (1994)	21.99	–	–	–	–
Shu and Wang (1999)	22.42	49.93	55.51	82.32	99.64
Wei et al. (2001)	22.42	49.88	55.54	82.26	99.67
Ex. 5					
Present FEM	28.37	52.26	67.64	89.74	100.2
Keer and Stahl (1972)	28.37	–	–	–	–
Rao et al. (1973)	28.62	–	–	–	–
Narita (1981)	28.44	53.49	67.85	90.50	100.6
Fan and Cheung (1984)	28.65	54.00	68.58	–	–
Wei et al. (2001)	28.36	53.29	67.60	89.87	100.4
Ex. 8					
Present FEM	25.74	58.03	58.03	97.45	101.4
Narita (1981)	26.18	58.70	58.70	98.58	102.0
Liew et al. (1993)	24.72	56.97	–	96.37	100.6
Wei et al. (2001)	26.66	56.90	62.30	96.33	105.3

Table 3
Frequency parameters Ω of *isotropic* square plates with mixed boundary conditions ($\nu = 0.3$)

	Ω_1	Ω_2	Ω_3	Ω_4	Ω_5
Ex. 1					
Present FEM	2.759	6.200	14.15	23.48	26.73
Ex. 3					
Present FEM	5.271	18.85	23.96	39.74	51.83
Ex. 4					
Present FEM	17.05	17.23	34.03	40.27	40.27
Ex. 6					
Present FEM	17.16	30.80	40.27	56.51	68.06
Ex. 7					
Present FEM	25.03	52.27	52.27	71.07	87.58
Ex. 9					
Present FEM	25.19	52.28	54.59	75.00	91.72

symmetric 8-layer plates are chosen for comparison as $[0/0/0/0]_s$, $[90/90/90/90]_s$, $[0/90/0/90]_s$, $[30/-30/30/-30]_s$, $[45/-45/45/-45]_s$ and $[0/-45/45/90]_s$. The first three (i.e., $[0_4]_s$, $[90_4]_s$ and $[(0/90)_2]_s$) are macroscopically specially orthotropic. The next two ($[(30/-30)_2]_s$ and $[(45/-45)_2]_s$) are alternating angle-ply sequence, and the last one ($[0/-45/45/90]_s$) is a quasi-isotropic case. The highest fundamental frequencies

Table 4
Illustration of a LO procedure for a symmetric 8-layer square plate (Ex. 2, $a/b = 1$, increment $\theta = 5°$)

	$[\theta_1/\theta_2/\theta_3/\theta_4]_s$	Ω_1
First iterative cycle of solutions		
Step 0	$[*/*/*/*]_s$	–
Step 1	$[70/*/*/*]_s$	44.72
Step 2	$[70/-50/*/*]_s$	57.87
Step 3	$[70/-50/50/*]_s$	61.80
Step 4	$[70/-50/50/50]_s$	62.32
Second iterative cycle of solutions		
Step 0	$[70/-50/50/50]_s$	62.32
Step 1	$[55/-50/50/50]_s$	63.17
Step 2	$[55/-50/50/50]_s$	63.17
Step 3	$[55/-50/-55/50]_s$	63.54
Step 4	$[55/-50/-55/55]_s$	63.54
Third iterative cycle of solutions (same as second)		

Table 5
Converged optimum solutions by a LO procedure for symmetric 8-layer square plates with mixed boundary conditions ($a/b = 1$, increment $\theta = 5°$, NIC: number of iterative cycle)

	$[\theta_1/\theta_2/\theta_3/\theta_4]_{s,\mathrm{opt}}$	$\Omega_{1,\mathrm{opt}}$	NIC
Ex. 1	$[70/70/60/-45]_s$	9.507	1
Ex. 2	$[55/-50/-55/55]_s$	63.54	2
Ex. 3	$[-70/45/-70/45]_s$	15.86	3
Ex. 4	$[70/-25/-45/-40]_s$	44.80	3
Ex. 5	$[90/85/-70/60]_s$	85.43	2
Ex. 6	$[85/0/-65/-5]_s$	46.57	4
Ex. 7	$[45/-45/-45/-45]_s$	65.64	1
Ex. 8	$[45/-45/-45/-45]_s$	69.89	1
Ex. 9	$[45/-40/-45/-45]_s$	66.63	1

Table 6
Comparison between the optimum frequency $\Omega_{1,\mathrm{opt}}$ and reference frequencies Ω_1 of symmetric 8-layer square plates for six typical stacking sequences ($a/b = 1$)

	$\Omega_{1,\mathrm{opt}}$	$[0_4]_s$	$[90_4]_s$	$[(0/90)_2]_s$	$[(30/-30)_2]_s$	$[(45/-45)_2]_s$	$[0/-45/45/90]_s$
Ex. 1	9.507[a]	2.982	6.631	5.948	4.398	6.513	4.531
Ex. 2	63.54[a]	45.86	54.56	50.40	56.61	62.16	52.57
Ex. 3	15.86[a]	6.934	14.30	10.26	12.24	14.56	11.26
Ex. 4	44.80[a]	19.76	33.12	37.29	27.85	37.79	31.56
Ex. 5	85.43[a]	49.15	85.30	63.99	62.44	72.83	60.87
Ex. 6	46.57[a]	21.29	33.19	40.23	32.98	40.91	33.92
Ex. 7	65.64[a]	47.94	47.94	60.18	61.04	65.35	60.68
Ex. 8	69.89[a]	57.03	57.03	61.11	67.09	69.56	64.40
Ex. 9	66.63[a]	51.13	47.96	60.60	63.55	66.27	62.27

[a] Maximum frequency value in the same example.

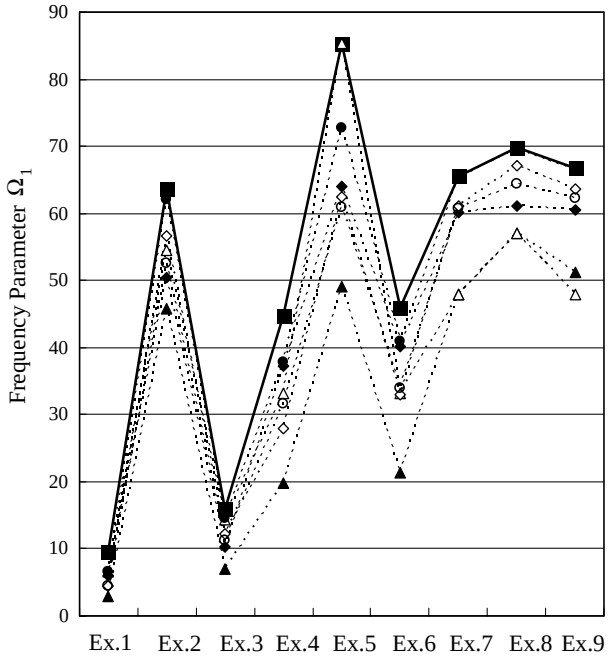

Fig. 4. Comparison between the optimum frequency parameter $\Omega_{1,opt}$ and frequency parameters Ω_1 of symmetric 8-layer square plates with six different lay-ups, ■: Present optimum frequency $\Omega_{1,opt}$, ▲: $[0_4]_s$, △: $[90_4]_s$, ♦: $[(0/90)_2]_s$, ◇: $[(30/-30)_2]_s$, ●: $[(45/-45)_2]_s$, ○: $[0/-45/45/90]_s$ (quasi-isotropic).

among those with the same boundary condition in the table are denoted by [a] and it is observed that all the present optimum solutions yield higher frequency values than those of plates with other stacking sequences.

The optimum of the present solutions is also corroborated graphically in Fig. 4, wherein the present solutions are compared to the reference values. In the figure, specially orthotropic plates, $[0_4]_s$ and $[90_4]_s$ are denoted by ▲ and △, respectively, and $[(0/90)_2]_s$ is by ♦. The alternating angle-ply sequences $[(30/-30)_2]_s$ and $[(45/-45)_2]_s$ are denoted by ◇ and ●, respectively. The last quasi-isotropic case $[0/-45/45/90]_s$ is by ○. It is clearly seen in the figure that the present optimum solutions (denoted by ■) yield higher fundamental frequencies than any of those plates with typical stacking sequences. The differences between the maximum and minimum frequencies are less significant in the first group (Ex. 1–3).

Structural applications of composite rectangular plate may involve various aspect ratios and it is of practical interest to examine whether an LO procedure works or not for different aspect ratios. For the purpose, Table 7 presents results of optimum solutions for Ex. 2 in the case of aspect ratios ranging from $a/b = 1/3$ to 3. In the table, the angle $\theta = 0$ in layers is dominant for $a/b = 1/3$ and 1/2 because the fibers (the major material axis) are directed to bridge the short span between a pair of opposite simply supported edges. For large aspect ratios, say $a/b = 2$ and 3, the partial clamped edge still has an effect to slant the optimum fiber angles from $\theta = 90°$. The optimum of these solutions (Ex. 2) is demonstrated for various aspect ratios in Fig. 5 by illustrating that the optimum frequency parameters $\Omega_{1,opt}$ are all higher than those with other typical stacking sequences. The same symbols as in Fig. 4 are used for various stacking sequences. In presenting the frequencies, the parameter Ω_1 is divided by a/b so that the modified parameters $\Omega_1/(a/b)$ give the frequencies for the plates with an equivalent plate area. It is observed again that the present optimum frequencies are all higher that those with other stacking sequences.

Table 7
Converged optimum solutions for Ex. 2 by a LO procedure for symmetric 8-layer rectangular plates with various aspect ratios (increment $\theta = 5°$, NIC: number of iterative cycle)

a/b	$[\theta_1/\theta_2/\theta_3/\theta_4]_{s,\mathrm{opt}}$	$\Omega_{1,\mathrm{opt}}$	NIC
1/3	$[0/0/0/0]_s$	39.24	1
1/2	$[0/0/0/5]_s$	40.08	1
2/3	$[-25/35/35/30]_s$	42.72	4
1	$[55/-50/-55/55]_s$	63.54	2
3/2	$[65/-65/65/65]_s$	116.0	2
2	$[65/-65/70/70]_s$	183.7	3
3	$[90/85/-85/70]_s$	366.1	1

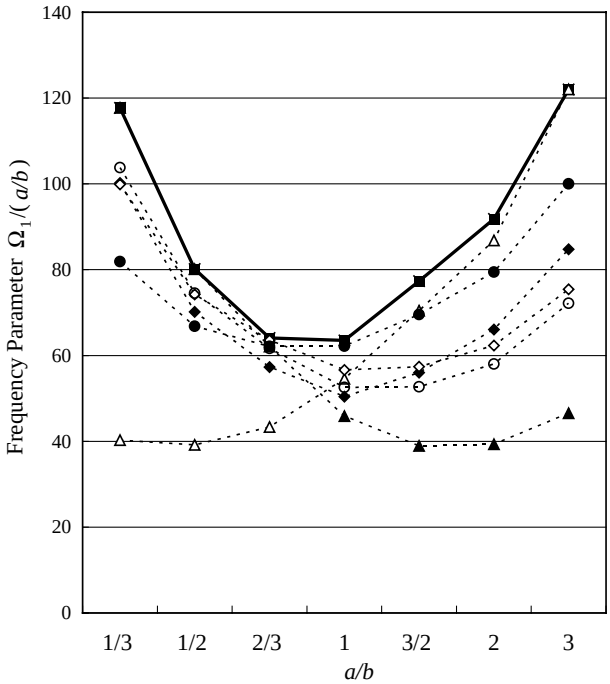

Fig. 5. Comparison between the optimum frequency parameter $\Omega_{1,\mathrm{opt}}/(a/b)$ and frequency Parameters $\Omega_1/(a/b)$ of symmetric 8-layer square plates (Ex. 2) with seven different aspect ratios; Present optimum frequency $\Omega_{1,\mathrm{opt}}$, ▲: $[0_4]_s$, △: $[90_4]_s$, ♦: $[(0/90)_2]_s$, ◇: $[(30/-30)_2]_s$, ●: $[(45/-45)_2]_s$, ○: $[0/-45/45/90]_s$ (quasi-isotropic).

In Table 8, the maximum fundamental frequencies and their corresponding fiber orientation angles are presented to show the effectiveness of the LO approach even for plates with many layers. This example represents the fact that even very thin layers (i.e., with the layer thickness obtained by dividing the plate thickness by 24) can make the difference in bending stiffness enough to allow the layerwise optimization to work well. The optimum frequencies are compared to the frequencies of the plates with typical lay-ups of $[0_{12}]_s$, $[(0/90)_6]_s$, $[(45/-45)_6]_s$ and $[(0/-45/45/90)_3]_s$, and have the highest frequency values in all the cases. It is also interesting to compare the optimum fiber orientation angles of the 24-layer plates with those of the 8-layer plates in Table 5. Direct comparison of the solutions is possible for both plates with different number of layers, since the frequency parameter Ω is normalized with the plate thickness. In

Table 8
Converged optimum solutions and reference frequencies of symmetric 24-layer square plates for four typical stacking sequences ($a/b = 1$, increment $\theta = 15°$)

	Ω_1					
	Ω_{opt}	$[0_{12}]_s$	$[(0/90)_6]_s$	$[(45/-45)_6]_s$	$[(0/-45/45/90)_3]_s$	$[\theta_1/\theta_2/\theta_3/\theta_4/\theta_5/\theta_6/\theta_7/\theta_8/\theta_9/\theta_{10}/\theta_{11}/\theta_{12}]_s$,opt, (NIC)
Ex. 1	9.563[a]	2.982	6.528	6.402	6.395	$[75/60/75/75/75/75/30/90/45/60/30/75]_s$, (NIC = 2)
Ex. 2	63.16[a]	45.86	51.91	62.67	56.48	$[60/-45/60/60/-60/-60/60/60/60/60/60/60]_s$, (NIC = 2)
Ex. 3	15.84[a]	6.934	11.23	14.92	13.04	$[-75/45/45/-60/-60/-60/-60/-60/45/60/-60/45]_s$, (NIC = 3)
Ex. 4	45.22[a]	19.76	40.40	38.43	41.02	$[-60/45/90/0/60/-60/-15/60/-30/60/75/-45]_s$, (NIC = 1)
Ex. 5	85.42[a]	49.15	68.91	74.27	69.41	$[90/90/90/90/90/-75/60/-75/75/-75/75/75]_s$, (NIC = 1)
Ex. 6	46.51[a]	21.29	43.87	41.62	41.97	$[75/-15/90/90/0/-75/0/90/90/90/90/75]_s$, (NIC = 2)
Ex. 7	65.69[a]	47.94	60.82	65.65	64.03	$[45/-45/-45/45/-45/45/45/-45/45/-45/-45/30]_s$, (NIC = 1)
Ex. 8	69.96[a]	57.03	61.39	69.92	66.05	$[45/-45/-45/45/-45/45/45/-45/45/-45/-45/-45]_s$, (NIC = 1)
Ex. 9	66.66[a]	51.13	61.01	66.59	64.70	$[45/-45/-45/30/45/-45/-45/45/-45/45/45/30]_s$, (NIC = 1)

[a] Maximum frequency value in the same boundary condition.

theory, the optimum frequencies of the 24-layer plates should be slightly higher than those of the 8-layer plates for the same increment in θ, because the 24-layer plates have more design degree of freedom, i.e. more number of design variables, than the 8-layer plates. This tendency is observed in most cases, but due to the different increment ($\theta = 5°$ and 15°) the maximum difference is found in Ex. 2 where $\Omega_{1,opt}$ of the 8-layer plate is only 0.6 percent higher than $\Omega_{1,opt}$ of the 24-layer plate.

4. Conclusion

It has been demonstrated that the layerwise optimization approach, taking the finite element method into the process of calculating the object function, is numerically efficient and practical for optimizing the vibration behavior of laminated composite plates. To the author's knowledge, this is the first publication to have solved the optimum design problem for vibrating laminated composite plates with mixed boundary conditions. It is hoped that the LO approach, coupled with the FEM analysis, provides designers with a powerful means for developing the tailoring applications in composite structural design.

References

Fan, S.C., Cheung, Y.K., 1984. Flexural free vibrations of rectangular plates with complex support conditions. Journal of Sound and Vibration 93, 81–94.

Fukunaga, F., Sekine, H., Sato, M., 1994. Optimal design of symmetrically laminated plates for the fundamental frequency. Journal of Sound and Vibration 171, 219–229.

Gorman, D.J., 1984. An exact analytical approach to the free vibration analysis of rectangular plates with mixed boundary conditions. Journal of Sound and Vibration 93, 235–247.

Gurdal, Z., Haftka, R.T., Hajela, P., 1999. Design and Optimization of Laminated Composite Materials. Wiley-Interscience.

Jones, R.M., 1999. Mechanics of Composite Materials, second ed. Taylor & Francis.

Keer, L.M., Stahl, B., 1972. Eigenvalue problems of rectangular plates with mixed edge conditions. Journal of Applied Mechanics 39, 513–520.

Laura, P.A.A., Gutierrez, R.H., 1994. Analysis of vibrating rectangular plates with nonuniform boundary conditions by using the differential quardrature method. Journal of Sound and Vibration 173, 702–706.

Liew, K.M., Hung, K.C., Lam, K.Y., 1993. On the use of the substructure method for vibration analysis of rectangular plates with discontinuous boundary conditions. Journal of Sound and Vibration 163, 451–462.

Mizusawa, T., Leonard, J.W., 1990. Vibration and buckling of plates with mixed boundary conditions. Engineering Structures 12, 285–290.

Narita, Y., 1981. Application of a series-type method to vibration of orthotropic rectangular plates with mixed boundary conditions. Journal of Sound and Vibration 77, 345–355.

Narita, Y., 2003. Layerwise optimization for the maximum fundamental frequency of laminated composite plates. Journal of Sound and Vibration 263, 1005–1016.

Narita, Y., Turvey, G.J., 2004. Maximizing the buckling loads of symmetrically laminated composite rectangular plates using a layerwise optimization approach. IMechE, Journal of Mechanical Engineering Science 218 (Part C), 681–691.

Ohta, T., Hamada, M., 1963. Fundamental frequencies of simply supported but partially clamped square plates. Bulletin of Japan Society of Mechanical Engineers 6, 397–403.

Rao, G.V., Raju, I.S., Murthy, T.V.G.K., 1973. Vibration of rectangular plates with mixed boundary conditions. Journal of Sound and Vibration 30, 257–260.

Shu, C., Wang, C.M., 1999. Treatment of mixed and nonuniform boundary conditions in GDQ vibration analysis of rectangular plates. Engineering Structures 21, 125–134.

Wei, G.W., Zhao, Y.B., Xiang, Y., 2001. The determination of natural frequencies of rectangular plates with mixed boundary conditions by discrete singular convolution. International Journal of Mechanical Sciences 43, 1731–1746.

Vinson, J.R., Sierakowski, R.L., 1986. The Behavior of Structures Composed of Composite Materials. Martinus Nijhoff, Dordrecht.

Zienkiewicz, O.C., Taylor, R.L., 1991. The Finite Element Method, fourth ed. McGraw-Hill, New York.